JOURNAL OF CATALYSIS 145, 37–53 (1994)

The Chemistry of Acetates on the Rh(111) Surface

C. J. Houtman, N. F. Brown, and M. A. Barteau

Center for Catalytic Science and Technology, Department of Chemical Engineering, University of Delaware, Newark, Delaware 19716

Received January 8, 1993; revised August 10, 1993

The formation of acetates by the dissociation of acetic acid on the clean Rh(111) surface and by reactions of acetic acid, acetaldehyde, and ethanol with preadsorbed oxygen atoms was examined using HREELS and TPD. Acetate intermediates were identified by the characteristic vibrations of the O–C–O moiety symmetrically bonded to the surface via both oxygen atoms. Acetates formed from acetic acid on the clean Rh(111) surface decomposed via two pathways. C–O scission by 278 K released adsorbed carbon monoxide and atomic oxygen; decarboxylation at 372 K liberated carbon dioxide and hydrogen. Acetates were formed after the adsorption of both ethanol and acetaldehyde on the Rh(111)-(2 × 2)O surface, as well as after the adsorption of acetic acid. For the alcohol and the aldehyde, the adsorbed intermediate involved in the reaction with atomic oxygen was likely η^2(C,O)–acetaldehyde. For acetic acid on the Rh(111)–(2 × 2)O surface, acetates were formed via direct transfer of the acid hydrogens to the surface oxygen atoms to form surface hydroxyls. When oxygen atoms were present on the surface, the only pathway for acetate decomposition was decarboxylation at 430 K. Thus coadsorbed oxygen atoms provide significant stabilization of acetates on Rh(111), as previously observed for formates on the same surface. In the presence of adsorbed oxygen, a portion of the methyl groups of surface acetates was oxidized to CO at temperatures below those expected for reactions of atomic carbon and oxygen species. This observation suggests that oxygen intervenes in the acetate decomposition pathway prior to the complete fragmentation of these intermediates.

INTRODUCTION

Carboxylate intermediates are ubiquitous in catalysis. They are thermally stable, decomposing above room temperature on metal oxides and all but a few metals (1, 2). They are easily detected by vibrational spectroscopies, owing to the large extinction coefficients of modes associated with vibrations and deformations of the carboxyl group. Reactions of carboxylic acids, especially the simplest, formic acid (HCOOH), have been a common probe of both supported catalysts and single crystals. The correlation of metal catalyst activity with the thermodynamic properties of adsorbates to construct "volcano plots" has been perhaps best exemplified by the kinetics of formic acid decomposition since its exposition by Rootsaert and Sachtler (3). The selectivity of carboxylic acid decomposition has also been correlated with catalyst electronic properties, and carboxylates have been implicated as intermediates in a host of catalytic processes including water–gas shift (4–6), methanol synthesis (7–10), higher oxygenate synthesis (11, 12), selective and unselective oxidations (13, 14), ketone formation (15, 16), and various condensations (17).

If the familiarity of these intermediates has not bred contempt, it has at least produced an overestimate of our understanding of them. For example, 30 years after the appearance of the volcano plot for formic acid decomposition activity on metals, it was demonstrated (2) that linear free energy relationships can be constructed for formate decomposition (as implied by the volcano plot) but that different LFERs apply to the Group VIII and Ib metals (invalidating the correlation of the catalytic activities of both series of metals with a *single* volcano). A further striking aspect of the surface science results is that one need not consider the selectivity of formate decomposition in constructing or applying these LFERs for the kinetics of that reaction. This implies that the selectivity (to CO vs CO_2 in the case of formate decomposition) is determined by processes which occur *after* the transition state for formate decomposition. The same conclusion has been reached by Iglesia and Boudart (18) from studies of the catalytic reactions of formic acid on supported Ni and Ni–Cu alloy catalysts.

The nature of the participation by carboxylates becomes less certain as the complexity of the catalyst and the chemistry occurring on it increases. The stability of these ligands and their ease of detection lead to their implication as suspected intermediates in processes in which they may be mere spectators. For example, studies of the water–gas shift reaction on Cu-based catalysts have proposed both formate-mediated pathways and the absence of such pathways as kinetically significant contributors to the overall mechanism. While much evidence has been presented on both sides, recent kinetics measurements support the "surface redox" rather than the "formate" mechanism (19–21).

The role of formates and higher carboxylates in oxygen-

0021-9517/94 $5.00

ate synthesis from CO and H_2 is even less clear. Although these intermediates are frequently detected on supported metal catalysts, their location, their origin, and their contributions to the conversion of reactants to products remain to be defined. For example, in the case of methanol synthesis with palladium catalysts, both the Tamaru (22) and Ponec (23) groups proposed that zero-valent palladium does not produce methanol. The latter group demonstrated a positive correlation between methanol synthesis activity and the concentration of extractable Pd^+ ions on the catalyst; the former group correlated methanol synthesis activity with the population of formate species (detected by infrared spectroscopy) which might be expected to be formed at such oxidized metal centers. However, other reports (24–26) have questioned these conclusions. Studies on palladium single crystals in particular have shown that (i) zero-valent palladium *will* make methanol from CO and H_2 and (ii) methanol decomposition to CO + H_2 (and by inference from microscopic reversibility, methanol synthesis) does not proceed via formates on clean palladium (26). These observations implicate the oxide support rather than the metal as the binding site of the formate species detected spectroscopically; however, the site of their formation and the extent of their participation in the overall reaction scheme are less easily resolved.

This uncertainty increases as one proceeds to the synthesis of higher oxygenates, as both the reaction network (and the slate of potential side reactions) and the catalyst formulation increase in complexity. This chemistry and the role of acetates in it has recently been reviewed by Bowker (11), who concluded that acetates are active intermediates central to oxygenate synthesis. A variety of supporting and contradicting evidence can be found. Naito *et al.* (9) demonstrated a correlation between the activity of supported rhodium catalysts for higher oxygenate synthesis and the intensity of acetate bands in the infrared spectrum of these catalysts. When metals such as Rh and Pd were supported on relatively noninteracting supports such as SiO_2 or Al_2O_3, the oxygenate production activity and the carboxylate coverage were very low, but the addition of sodium as a promoter increased the level of both (9, 10). By the use of isotopically labeled CO, Naito *et al.* (9) determined that the oxygen atoms associated with sodium promoter atoms were responsible for the formation of carboxylates on the surface. When rhodium was supported on a more strongly interacting oxide, TiO_2, the catalysts did not require a promoter; simple oxygen treatment enhanced the oxygenate formation rate. This rate enhancement remained unchanged during a prolonged reaction period. This result suggests that TiO_2 can make oxygen available to the metal surface. The migration of titanium oxides onto Rh particles has been observed directly in the electron micrographs of Logan *et al.* (27). This migration may explain the formation of carboxylates on the surface of Rh/TiO_2 catalysts. Since in both of these examples decoration of the Rh surface with metal oxides enhances carboxylate formation, this reaction may occur at the interface between the metal and the support or promoter oxide.

While the apparent implication of the results of the studies of Naito *et al.* is that carboxylates are important intermediates in oxygenate production, one cannot rule out the possibility that they are spectator species derived in parallel or series with other oxygen-containing products. Solymosi and co-workers (28, 29) have suggested that the carboxylates are formed solely on the oxide support and do not participate significantly in the production of oxygen-containing products. These workers proposed that hydrogen, activated on Rh, migrates to the support where it reacts with CO to produce formate intermediates on Rh/SiO_2 catalysts. Higher carboxylates could be formed on the support by similar routes, or by reactions of the product aldehydes and alcohols, possibly produced at other sites.

The role that carboxylates play in CO hydrogenation and higher alcohol formation is the subject of ongoing study. Several issues involving carboxylate intermediates merit further investigation. Clearly the oxygen atoms associated with the support or promoter are involved in the formation of these intermediates from synthesis gas. If carboxylates are active intermediates, then the profound effects of support identity on catalyst activity and selectivity may be partially understood by studying the reactions and stability of these intermediates on the individual catalyst components in the presence and absence of oxygen and other modifiers. The focus of the present study was the stability and reactions of acetate intermediates on the Rh(111) surface. The acetate intermediates were formed via the dissociation of acetic acid on the clean surface and by the reaction of acetic acid, acetaldehyde, or ethanol with adsorbed oxygen atoms. The mechanisms of acetate formation and decomposition are considered.

EXPERIMENTAL

Experiments were carried out in an ion- and diffusion-pumped vacuum chamber previously described (30, 31). This instrument was equipped with a HREEL spectrometer (McAllister Technical Services), four grid optics (Physical Electronics) for AES and LEED, and a quadrupole mass spectrometer (UTI 100C) multiplexed with an IBM XT. The mass spectrometer ionizer was enclosed by a quartz shroud with a 7-mm-diameter hole at the entrance and two side vents. This shroud enhanced the collection of products in TPD experiments and minimized the sensitivity to species desorbed from the crystal support hardware.

The polished, (111)-oriented Rh single crystal was spot-

welded onto two 0.5-mm tantalum wires that served as supports as well as heating elements when a current was supplied. The crystal was cooled to ca. 85–90 K by thermal conduction through a 0.64-cm copper feedthrough, the opposite side of which was immersed in liquid nitrogen. The temperature of the Rh(111) sample was monitored with a chromel–alumel thermocouple spot-welded to the back. The sample was cleaned by cycles of ion bombardment, oxygen TPD, and annealing to 1400 K. The surface produced by this treatment was determined to be clean using AES, HREELS, and oxygen TPD.

The acetic acid, acetaldehyde, and ethanol samples were stored in separate glass tubes attached to a stainless-steel manifold by all-metal valves. These samples were purified by repeated freeze/pump/thaw cycles, and were dosed onto the crystal via a 1.5-mm stainless-steel needle attached to the dosing line. Following the adsorption of the reactants and the recovery of the chamber background pressure, either TPD or HREELS experiments could be carried out. In TPD experiments the sample temperature was linearly ramped (4.0 ± 0.2 K/s) under computer control, and up to eight mass fragments of the desorbing products were monitored with the multiplexed mass spectrometer. In HREELS experiments, spectra were typically obtained for specular reflection of a 5-eV electron beam from the surface. The typical height and width of the elastically scattered beam were 6.5×10^5 counts/s at a FWHM of 70 cm^{-1}. Temperature-programmed steps between HREELS experiments were also carried out at 4 K/s. When the desired temperature had been reached, the power supply was turned off and the crystal was allowed to cool to the initial temperature before collection of each HREEL spectrum.

The yields of the individual products in TPD experiments are reported below to two significant figures in units of monolayers (ML). These were determined as follows. The mass spectrometer signals for the eight fragments monitored concurrently during each TPD experiment were first corrected for overlapping contributions from multiple products. Such corrections were relatively minor in this case because of the simplicity of the product distribution. Essentially the only significant correction was the removal of the small $m/e = 28$ contribution due to CO_2 cracking from the $m/e = 28$ signal assigned to CO. Since the CO and CO_2 peaks were separated in temperature, this operation had a negligible effect on CO peak shapes. Next the area under the TPD spectrum for each product was determined by numerical integration. The precision of the coverage calculations reflects the precision of this integration; all other errors are systematic ones contained in the calibrations of mass spectrometer sensitivity factors applied to these data. The area of the CO desorption peak was converted to surface coverage in monolayer units by normalization against the peak area obtained after adsorbing molecular CO to a coverage of 0.33 ML to produce a $\sqrt{3} \times \sqrt{3}$ R30° LEED pattern (32). One monolayer is defined as the number of rhodium atoms on the (111) surface, 1.62×10^{15} atoms/cm^2. The yields of all other products were determined by application of the mass spectrometer sensitivity factors, calculated by the method of Ko *et al.* (33) from fragmentation patterns experimentally determined for the apparatus used for the TPD experiments. The relative mass spectrometer sensitivities for H_2 and CO were determined by calibration of the signals for these products as in previous TPD results for the stoichiometric decomposition of methanol on the Rh(111) surface (34). The amount of carbon deposited on the surface after each TPD experiment was determined by integration of the signals for CO and CO_2 produced in a second TPD experiment in which oxygen was adsorbed on the surface to burn off this carbon. These values are subject to somewhat greater uncertainty than those for other products, since they were not obtained simultaneously and may be influenced by slight variations in pumping speed and other conditions from run to run. However, as demonstrated in this and in previous studies of oxygenate chemistry on Rh surfaces (31, 34–38), excellent mass balance closure was obtained by following these procedures.

RESULTS

Acetic Acid on the Rh(111) Surface

Acetic acid adsorbed intact on the Rh(111) surface at 89 K. The vibrational bands associated with this molecular species dominate the 89-K spectrum of Fig. 1a. The strongest evidence for molecular acetic acid was the very close agreement between this spectrum and the spectrum obtained on Pd(111) (39). Davis and Barteau observed a weak ν(OH) mode at 2525 cm^{-1}. The identification of this mode was evidence for molecular acetic acid on this surface at 170 K. The frequency they observed for this mode was 1058 cm^{-1} below the gas-phase value of 3583 cm^{-1}. The formation of catemers via hydrogen bonding was the reason for this large downward shift in frequency. The O–H modes of formic acid on the Rh(111) surface were also perturbed relative to those in the gas phase. The ν(OH) frequency shifted from 3570 cm^{-1} in the gas phase to two peaks, at 2575 and 2700 cm^{-1}, for formic acid on the Rh(111) surface (35). The modes associated with the O–H bond of adsorbed acetic acid were also observed at ca. 2500 and 2700 cm^{-1} on Rh(111). The vibrational assignments for gaseous acetic acid (40) and acetic acid adsorbed on Rh, Pd (39), and Cu (41) are summarized in Table 1. Bowker and Madix (42) have shown by UPS that acetic acid bonded to the Cu(110) surface via the lone pair electrons on the oxygen of the OH group. The bonding via the lone pair electrons on this oxygen atom

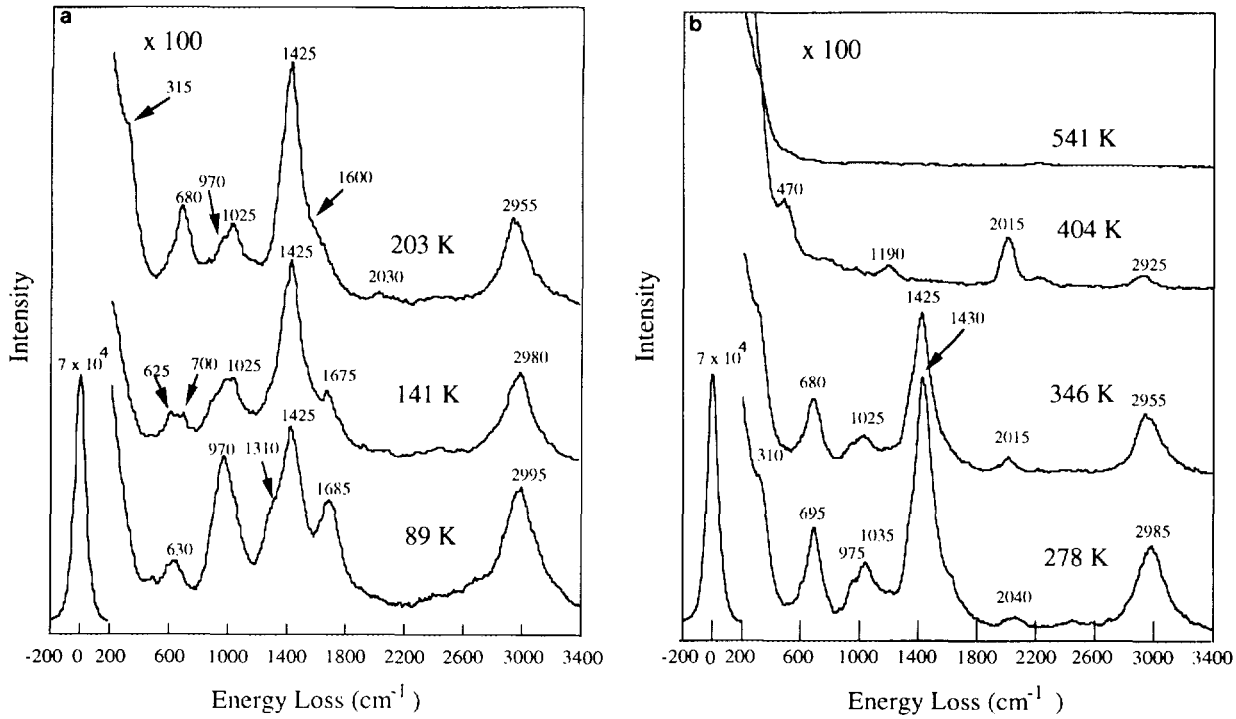

FIG. 1. (a) HREELS after an exposure of 1.1 L of acetic acid at 89 K, and HREELS after subsequent heating to 141 and 203 K. (b) HREELS after subsequent heating to 278, 346, 404, and 541 K.

has been widely proposed for other oxygenates, including alcohols, ketones and ethers.

Heating the surface to 141 K resulted in changes in the spectrum that signaled the formation of acetate intermediates had begun. Comparing the 141- and 89-K spectra of Fig. 1a, the decrease in intensity of the ν(C–O) and ν(C=O) modes at 1310 and 1685 cm^{-1}, respectively, and the increase in intensity of the ν_s(OCO) mode at 1425 cm^{-1} showed that the conversion of acetic acid to acetates was underway. The decrease in intensity of the ν(C–C) mode at 970 cm^{-1} was the most obvious change. This reaction continued until 203 K where the ν(C=O) mode was completely eliminated, and modes characteristic of acetates were observed. The assignments of the vibrational frequencies of the acetates are summarized in Table 2. Similar modes have been observed for the formate intermediate produced by warming formic acid adsorbed on the Rh(111) surface to 178 K (35). The vibrational frequencies for the formate intermediate were 790 cm^{-1} for the δ(O–C–O) and 1330 cm^{-1} for the ν_s(O–C–O) modes. The significant differences in the frequencies of the O–C–O modes of acetates and formates is the result of a coupling of carboxyl modes with the ν(C–C) mode of acetates not possible for formates. A shoulder was also

TABLE 1

Acetic Acid HREELS Assignments, Frequency (cm^{-1})

Mode	Gas phase (40)	Rh	Pd (39)	Cu (41)
$\nu(CH_3)$	2996/2944	2995	2965	3005
ν(OH)	3583	2700/2500	2525	3005
ν(C=O)	1788	1685	1685	1670
$\delta(CH_3)$	1430/1382	1425	1425	1420
ν(C–O)	1180	1310	1310	1420
ν(C–C)	847	970	955	nr
δ(O–C–O)	657	630	685	690
Lattice	—	nr	250	288

Note. nr, not resolved.

TABLE 2

Acetate HREELS Assignments, Frequency (cm^{-1})

Mode	Sodium acetate (43)	Rh	Pd (39)	Cu (41)
$\nu(CH_3)$	3000	2955	2965	3040
ν_a(O–C–O)	1585	1600	nr	nr
$\delta(CH_3)$	1440	1425	1415	1480
ν_s(O–C–O)	1408	1425	1415	1480
$\rho(CH_3)$	1050/1009	1025	nr	1055
ν(C–C)	924	970	925	nr
δ(O–C–O)	645	680	685	700
$\nu(M$–O)	—	315	320	336

Note. nr, not resolved.

observed at ca. 1600 cm^{-1}. An IR band with a frequency of 1577 cm^{-1} was observed for acetates on Rh/SiO_2 catalysts (10). This IR band is associated with the ν_a(O–C–O) mode of acetates, and the shoulder in the HREEL spectrum was similarly assigned.

The HREEL spectra indicate that acetate intermediates decomposed at higher temperatures on Rh(111). As can be observed from Fig. 1b, CO began to appear by 278 K. CO was fingerprinted by its ν(C=O) vibration at 2040 cm^{-1}. The CO was apparently formed from the decomposition of acetate intermediates, since no other intermediate was detected on the surface prior to its formation. Specifically, the participation of acetic anhydride, as suggested by Bowker and Madix (42) for Cu(110), was not indicated in either the TPD or HREEL spectra. Heating the surface from 346 to 404 K resulted in the elimination of the modes associated with the acetate and an increase in the intensity of the losses for CO. At 404 K, besides modes indicative of carbon monoxide, peaks characteristic of surface bound hydrocarbons were also observed. The modes at 1190 and 2925 cm^{-1} were most likely due to methylene (CH_2) or methylidyne (CH) species produced during acetate decomposition. Similar losses were observed following CO elimination from ethylene oxide on this surface (44), a reaction which would also be expected to produce adsorbed methylenes. The vibrations of both CO and the surface-bound hydrocarbon fragments were eliminated by further heating to 541 K.

The decomposition of acetic acid was also studied by TPD. The TPD spectrum obtained after exposing the Rh(111) surface to 1.2 Langmuir (L) of acetic acid is illustrated in Fig. 2. This exposure was roughly sufficient to saturate the first layer. Higher exposures resulted in the desorption of acetic acid from a multilayer state at lower temperature. The absence of acetic acid desorption at a 1.0-L exposure indicated that adsorption in the first layer was irreversible. In contrast, Davis and Barteau (39) observed that acetic acid desorbed from the Pd(111) surface after exposures that did not saturate the acetate decomposition channels. They suggested that in addition to molecular desorption, acetic acid was also produced by the hydrogenation of acetate intermediates. Apparently the greater decomposition activity and lower hydrogenation activity of Rh prevents acetic acid from being produced at subsaturation coverages via either of the channels observed on Pd.

The acetates identified by HREELS decomposed between 278 and 404 K. In fact some CO was already detected in the 278 K spectrum. From Fig. 2, it can be observed that two products exhibited maximum desorption rates in this temperature range. The evolution of CO_2 and H_2 at 372 K was likely due to the decarboxylation of the acetate intermediates. The TPD yield of CO_2 indicated that 0.093 monolayers (ML) of acetate decomposed via

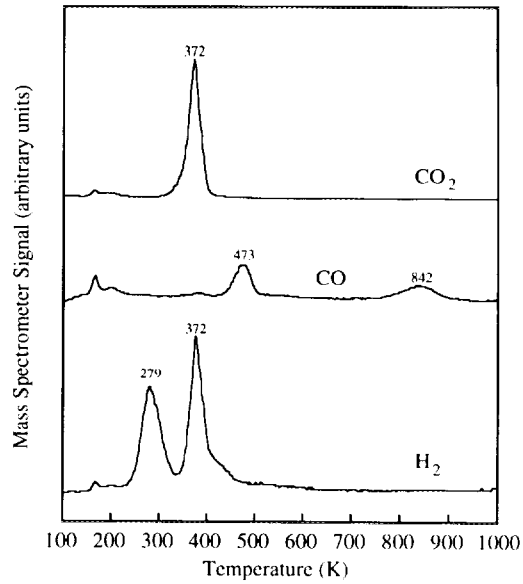

FIG. 2. TPD after an exposure of 1.2 L of acetic acid at 89 K. Yields corresponding to this spectrum are given in Table 3.

this route. The hydrogen desorption peak at 372 K corresponded to 0.14 ML of H_2. The ratio of H_2/CO_2 was 1.5, consistent with the acetate stoichiometry. The yields corresponding to Fig. 2 are summarized in Table 3. Although the fate of the methyl group was complete dehydrogenation to surface carbon, the bond-breaking sequence for acetate decomposition is not immediately apparent from the data of Fig. 2. There are two likely possibilities: either methyl groups are released to the surface by C–C bond cleavage, or hydrogen abstraction from the methyl group precedes C–C bond cleavage. No methane desorption was observed at this temperature in any case.

From our previous studies of acetaldehyde decarbonylation on Rh(111), methane was produced at 267 K with selectivities of up to 50% of the methyl groups released from saturation coverages of acetaldehyde (36). The selectivity for methane production was coverage dependent, however, at the lower coverages of acetic acid decom-

TABLE 3

TPD Yields (ML) for an Exposure of 1.2 L of Acetic Acid

H_2 (279 K)	0.10
H_2 (372 K)	0.14
CO_2 (372 K)	0.093
CO (473 K)	0.027
CO (842 K)	0.024
$C_{(ad)}$	0.093

posed, one would still expect methane selectivities of ca. 20% by comparison with acetaldehyde decomposition at comparable levels. This comparison would suggest that, unlike acetaldehyde decarbonylation at 267 K, acetate decarboxylation at 372 K does not occur by C–C scission to release intact methyl groups to the surface. If so, the acetate decarboxylation must proceed via an initial C–H scission at the methyl carbon; subsequent C–C scission would deposit methylenes or less hydrogen-rich C_1 species on the surface. The proper analogy would therefore be to the decarbonylation of ethoxides on Rh(111); these intermediates decompose via C–H scission of the β-carbon, releasing CO plus CH_2 or CH ligands, and produce *no* methane (36). The absence of methane formation from either acetic acid or ethanol on the Rh(111) surface may once again reflect the activity of this surface for activation of β-CH bonds by essentially an oxidative addition step. However, some caution must be exercised in drawing this analogy. Acetaldehyde decarbonylation occurs at temperatures below those at which the rate of hydrogen atom recombination is significant, thus methyl groups released from acetaldehyde encounter a relatively hydrogen-rich surface (the acyl hydrogen from acetaldehyde dissociation to acetyls remaining on the surface). The selectivity for methane formation from acetaldehyde can be manipulated somewhat by variation of the hydrogen availability (by preadsorption of additional hydrogen), however the selectivity is largely controlled by the competing irreversible decomposition of methyl groups to less-hydrogen-rich intermediates. If methyl groups were released by acetate decarboxylation at 372 K, the formation of methane could be suppressed by increased competition from both competing reactions above, relative to that experienced by CH_3 species *ex*-CH_3CHO at 267 K. Hydrogen atom recombination at 372 K is fast, as evidenced by the common shapes of the CO_2 and H_2 peaks at this temperature in Fig. 2. Thus the population of hydrogen atoms available for reaction with any CH_3 groups liberated would be much less for acetate decarboxylation at 372 K than that for acetaldehyde decarbonylation at 267 K. This would strongly disfavor the bimolecular surface reaction to form methane relative to the unimolecular decomposition of adsorbed methyl intermediates. Thus while the absence of methane production is consistent with the conclusion that acetate decarboxylation occurs by initial C–H scission, one cannot rule out the possibility on this basis alone that this reaction releases methyl groups whose reaction to methane is kinetically disfavored relative to competing processes.

In order to probe further the sequence of elementary processes for acetate decomposition on the Rh(111) surface, the decomposition of CD_3COOD was also examined. As for CH_3COOH, the only volatile carbon-containing products observed were CO and CO_2. The carbon monoxide peak appeared at its usual, desorption-limited position, 473 K, but the CO_2 peak from CD_3COOD was shifted upward in temperature to 409 K, 36 K higher than that from CH_3COOH. This shift in peak temperatures corresponds to an activation energy difference of 2.35 kcal/mol, if one assumes a preexponential factor of 10^{13} s^{-1} for the first-order decomposition of acetates. This activation energy difference would produce a ratio of rate constants for decomposition of CH_3COO vs CD_3COO of 18 at the temperature, 409 K, at which the deuterated species decomposes. The magnitude of this ratio is clearly indicative of a primary kinetic isotope effect for acetate decomposition, and demonstrates that the rate-determining step in this sequence is scission of a C–H (or C–D) bond. If C–H bond scission precedes C–C scission, acetate decomposition can deposit C_1 fragments on the surface which contain no more than two hydrogens each. Thus the kinetic isotope effect, the absence of methane, and the observation of the ca. 1200 cm^{-1} mode in the HREEL spectrum of the CH_3COOH adlayer at 404 K all lead to the same conclusion: acetate decarboxylation is initiated by C–H scission, and subsequent C–C scission releases CO_2 and deposits methylene (CH_2) moieties on the surface.

Returning to Fig. 2 and the TPD results for CH_3COOH, a second, lower temperature hydrogen peak was observed at 279 K. HREELS indicated that acetate intermediates were formed below 200 K. However, the desorption of H_2 from the reaction of H atoms produced at such temperatures is limited by kinetics of the recombination reaction, and typically exhibits an onset temperature of ca. 250 K as previously demonstrated for H_2 production from CH_3OH and H_2CO on Rh(111) (34, 35). Thus at least a portion of the hydrogen atoms in the 279 K peak in Fig. 2 were the result of acetate formation. This peak was equivalent to 0.10 ML of H_2. As shown in Fig. 2, CO desorbed at 473 K. From HREELS, it was shown that losses characteristic of CO were evident by 278 K. The amount of CO in the 473 K peak was 0.027 ML. If all the CO in this peak were due to acetate decomposition, then the stoichiometry would dictate that complete dehydrogenation of the acetates would release 0.081 ML of H atoms to the Rh(111) surface. Since the 372-K H_2 peak represents the H atoms lost in forming CO_2 from acetates, the H atoms released in forming CO must contribute to the 0.10 monolayers of H_2 desorbing at 279 K. Decomposition of the acetates to yield 0.027 ML of CO would yield 0.041 ML of H_2 at this temperature. Thus, the remaining 0.059 ML of H_2 must result from formation of the acetates. If 0.093 ML of CO_2 and 0.027 ML of CO resulted from acetate decomposition, then 0.12 ML of acetic acid dissociated to form the acetates. Dissociation of this amount of acetic acid released 0.06 ML of H_2. Approximately 40% of the hydrogen in the 279 K peak was therefore a result of acetate decomposition via the pathway that

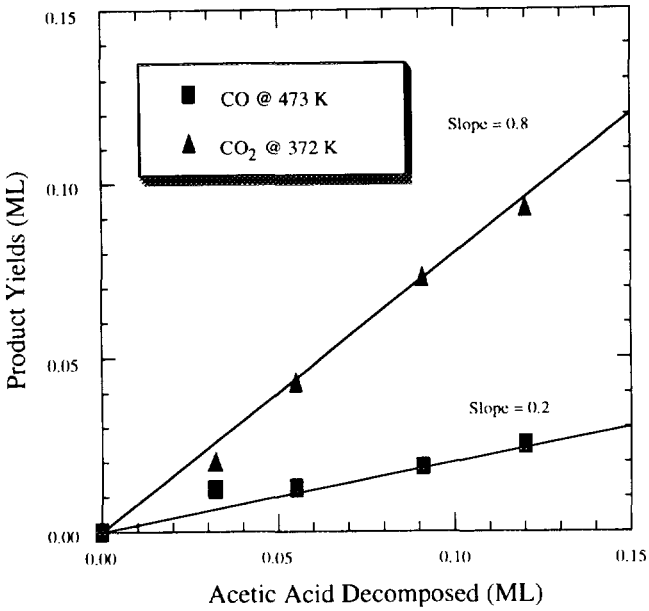

FIG. 3. Product yields for CO at approximately 473 K and CO_2 at approximately 372 K from acetic acid decomposition versus the total amount of acetic acid decomposed. Both the vertical axis and the horizontal axis have units of monolayers of molecules. A monolayer is defined as the number of Rh atoms in the top layer of the close-packed surface, 1.62×10^{15} atoms/cm^2.

produced CO. The remaining hydrogen was a result of the dissociation of acetic acid to acetates which was observed to occur at ca. 141 K in HREELS. A second CO desorption peak was also observed at 842 K. This peak was assigned to the reaction of atomic carbon and oxygen, since similar peaks were observed during the O_2 TPD experiments used to clean the surface. Although the peak shape was much lower and broader, the amount of CO represented by this higher temperature CO peak, 0.024 ML, was essentially the same as the amount in the CO peak at 473 K. Since the surface was initially clean, the oxygen atoms that were consumed to form CO at 842 K must have been the product of acetic acid or acetate decomposition at lower temperatures. The stoichiometry of acetate dictates that for every molecule of CO produced from acetate decomposition, an oxygen atom must also be released. Thus it is not surprising that the amount of CO in the two CO peaks was essentially the same. The methyl groups of surface acetates which decomposed by one of the two lower temperature pathways were the source of the carbon atoms consumed in this reaction with oxygen. There was also 0.093 ML of carbon left on the surface after the acetic acid experiments. This was determined by integrating the CO and CO_2 desorption peaks observed during subsequent oxygen TPD experiments.

Coverage variation studies were also performed in which different amounts of acetic acid were adsorbed on the Rh(111) surface. From these studies, it was determined that CO, CO_2, H_2, and $C_{(ad)}$ were the only products from acetic acid decomposition for all coverages of acetic acid. A plot of the yields of CO_2 at ca. 372 K and of the yields of CO at ca. 473 K versus the total amount of acetic acid decomposed (calculated from the oxygen content of the products) is shown in Fig. 3. It can be seen that approximately 80% of the acetic acid decomposed via decarboxylation to produce CO_2 while the other 20% decomposed via C–O bond cleavage to release CO. The CO_2/CO ratio of 4 : 1 from acetates is close to the ratio of 3 : 1 from formates (35). The main difference between acetate and formate decompositions is the absence of a low temperature CO_2 peak during decomposition of the acetates. Figure 4 shows a plot of the total yields of C and H atoms which were accounted for during the coverage variation experiments. At all coverages examined the yields for all three atoms were within 10% of the stoichiometric values, and for most points in Fig. 4 the agreement was within even narrower bounds.

In summary, TPD and HREELS experiments have shown that acetic acid adsorbed intact on the Rh(111) surface. Molecular acetic acid was converted to acetate intermediates beginning at 141 K. Approximately 20% of the acetate intermediates decomposed to give molecular CO which desorbed at 473 K. The oxygen resulting from this decomposition pathway reacted with surface carbon

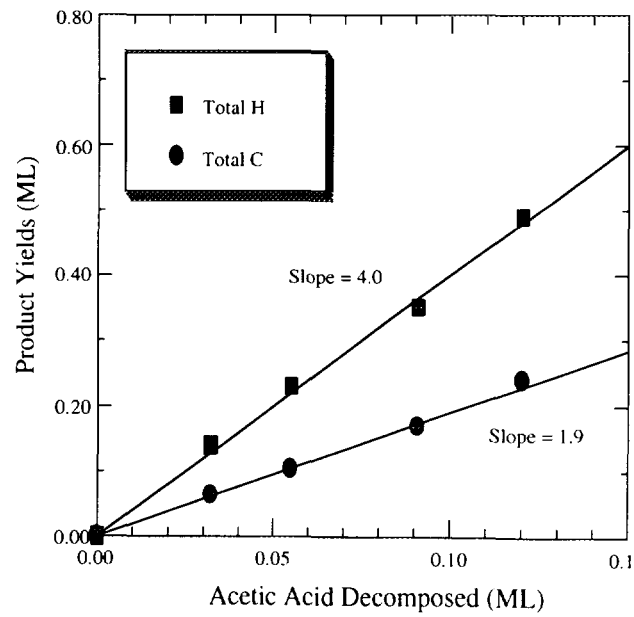

FIG. 4. Product stoichiometry for acetic acid decomposition versus the total amount of acetic acid that decomposed. Both the vertical axis and the horizontal axis have units of monolayers. A monolayer is defined as the number of Rh atoms in the top layer of the close-packed surface, 1.62×10^{15} atoms/cm^2.

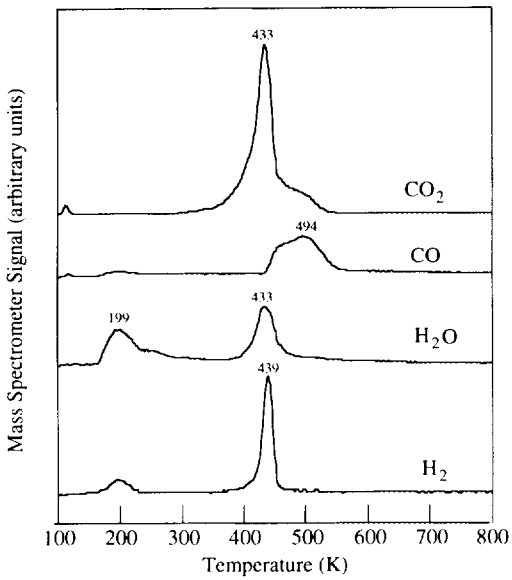

FIG. 5. TPD after an exposure of 1.5 L of acetic acid on the Rh(111)–(2 × 2)O surface at 90 K. Yields corresponding to this spectrum are given in Table 4.

to produce additional CO at 842 K. The decarboxylation of acetate intermediates was also observed at 372 K. This mode of decomposition accounted for the remainder of the acetic acid originally adsorbed. No methane was produced by acetate decarbonylation or decarboxylation; CO, CO_2, H_2 and adsorbed carbon were the only products.

Acetic Acid on the Rh(111)–(2 × 2)O Surface

The role of oxygen during acetic acid decomposition was also studied using TPD. The TPD spectrum obtained after exposing 1.5 L of acetic acid to a surface on which approximately 0.25 ML of oxygen atoms had been preadsorbed in a (2 × 2) configuration at 300 K is shown in Fig. 5. The H_2, H_2O, and CO_2 desorption peaks at 433 K were the products of the decomposition of the same intermediate since all appeared at the same temperature. This set of peaks is analogous to that observed for similar exposures of acetic acid on the clean surface. In that case, however, acetate decomposition occurred at 372 K and produced coincident peaks for H_2 and CO_2, but not H_2O. Desorption of molecular CO was also evident in both cases between 400 and 500 K. From HREELS it is shown that the intermediate decomposing to liberate H_2, H_2O, and CO_2 at 433 K on the oxygen-dosed surface was also acetate. The ca. 60 K increase in the acetate decomposition temperature is not surprising, as Solymosi *et al.* (45) observed that the addition of 0.25 ML of oxygen to a Rh(111) surface shifted the decomposition temperature of formate upward by 80 K. The total amounts of acetate decomposed on the two surfaces at saturation were quite similar: 0.12 vs 0.10 monolayers on the clean vs the (2 × 2) O surface.

The product yields for the reaction of acetic acid on the Rh(111)–(2 × 2) O surface are summarized in Table 4. From the TPD results, 0.052 ML of H_2O desorbed at 199 K. The desorption of water at this low temperature suggests that the removal of the acidic hydrogen from acetic acid involves the direct transfer to the oxygen adlayer, since the reaction of adsorbed oxygen and hydrogen atoms on this surface has been shown to require much higher temperatures, ca. 300 K (46). The observation of 0.052 ML of H_2O in the experiment of Fig. 5 is consistent with the formation of 0.10 ML of acetates by proton transfer from acetic acid below 200 K. Thus, the total amount of carbon contained in products liberated at higher temperatures from the decomposition of 0.10 ML of acetates would be expected to be 0.20 ML. At 433 K, 0.14 ML of CO_2 desorbed. Thus 0.06 ML of carbon atoms must either desorb as CO or remain on the surface as $C_{(ad)}$, since no hydrocarbon or oxygenate products were observed. Of this amount, 0.048 ML of CO was observed in a peak at 494 K, and 0.008 ML of $C_{(ad)}$ was detected by subsequent burn-off with oxygen. Thus, essentially all of the carbon was accounted for. Essentially all of the hydrogen was accounted for, also. Decarboxylation of the 0.10 ML of acetates should release H atoms at a ratio of H/C atoms of 1.5. The 0.074 ML of H_2O and the 0.051 ML of H_2 observed at ca. 433 K contain 0.24 ML of hydrogen atoms; thus the H/C ratio obtained was 1.3. This is in reasonable agreement with the expected value of 1.5.

The small amount of surface carbon detected in conjunction with the large amount of CO_2 desorbed implies that the surface oxygen also oxidized the products of acetate fragmentation, such as methylene groups and CO. The 0.10 ML of acetic acid decomposed contained 0.20 ML of oxygen atoms, but since 0.25 ML of oxygen atoms were adsorbed, the desorbing products should contain a total of 0.45 ML of oxygen atoms. The amount of oxygen in the products in Table 4 sums to approximately 0.45

TABLE 4

TPD Yields (ML) for an Exposure of 1.5 L of Acetic Acid on the Rh(111)–(2 × 2)O Surface

H_2O (199 K)	0.052
H_2 (439 K)	0.051
H_2O (433 K)	0.074
CO_2 (433 K)	0.14
CO (494 K)	0.048
$C_{(ad)}$	<0.008

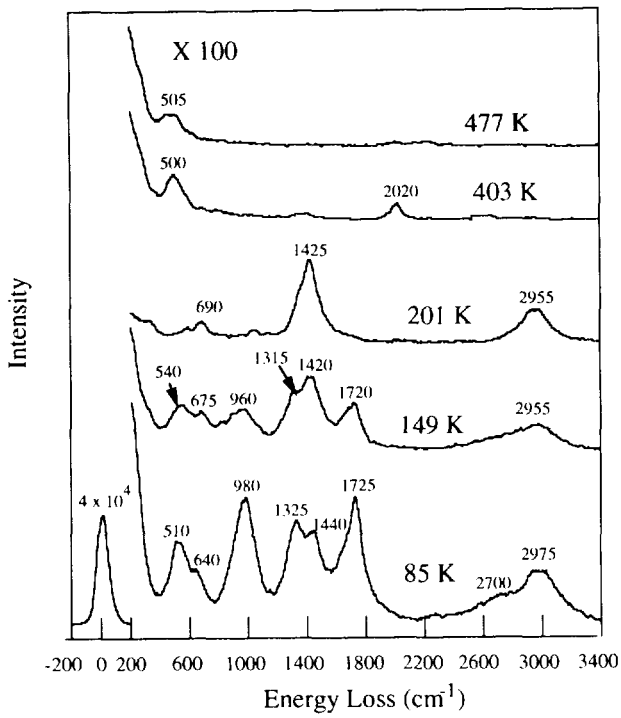

FIG. 6. HREELS after an exposure of 1.7 L of acetic acid on the Rh(111)–(2 × 2)O surface at 85 K, and HREELS after subsequent heating to 149, 201, 403, and 477 K.

ML, again indicating closure of the mass balance. It is surprising that the reaction between carbonaceous fragments and oxygen occurred at such low temperatures (below ca. 550 K), since on the clean surface the reaction between oxygen and carbon occurred at 842 K. Similar behavior has been observed for acetaldehyde on the oxygen-covered surface, as shown below. These results suggest that oxygen intervenes in the acetate decomposition pathway prior to complete fragmentation; in other words, the carbon atom originally contained in the methyl group of the acetate is not deposited on the surface as $C_{(ad)}$ before being oxidized. It is possible that oxygen reacts directly with adsorbed acetates, as well. Sault and Madix (47), for example, demonstrated by isotopic labelling experiments that oxidation of acetates on Ag(110) occurs by nucleophilic attack of oxygen on the methyl group prior to C–C scission.

From HREELS, it can be shown that acetic acid adsorbed intact on the oxygen-covered Rh(111) surface at 85 K. Vibrational bands associated with the molecular acetic acid were quite prevalent in the 85-K spectrum shown in Fig. 6. A band characteristic of the ν(Rh–O) mode was also observed at 510 cm^{-1}. As for acetic acid on the clean Rh(111) surface, a weak but broad mode at 2700 cm^{-1} was observed, although there was less intensity below 2600 cm^{-1} than for acetic acid on the clean surface. On both surfaces, peaks in this frequency range were ν(OH) modes of the acid perturbed by adsorption and by intermolecular hydrogen bonding. A comparison of the modes for acetic acid on the clean Rh(111) surface and on the oxygen-covered Rh(111) surface is shown in Table 5.

Heating the crystal to 149 K resulted in major changes in the spectrum. The most notable was the decrease in the ν(C–O) and the ν(C=O) modes at 1325 and 1725 cm^{-1}, respectively, and an increase in the ν(O–C–O) mode at 1425 cm^{-1}. By 149 K, the conversion of acetic acid to acetate species had clearly begun. By 201 K, the ν(C=O) mode at 1725 cm^{-1} was completely eliminated. In fact the predominant modes were the ν(O–C–O) mode, the δ(O–C–O) at 690 cm^{-1} and the $\nu(CH_3)$ mode at 2955 cm^{-1}. The spectrum at 201 K represents surface-bound acetate intermediates. No further changes were observed until 403 K. From the 403-K spectrum, it can be seen that modes characteristic of acetates disappeared as CO appeared in the spectrum. The mode at 2020 cm^{-1} is indicative of the ν(C=O) mode of carbon monoxide. The spectrum at 477 K shows that CO was removed and only a mode at ca. 500 cm^{-1} arising from trace amounts (see Table 4) of surface carbon or oxygen remained.

In summary, the TPD and HREELS spectra obtained for acetic acid and oxygen coadsorption showed that the hydroxyl hydrogen of the acid reacted with the surface oxygen to form hydroxyls which underwent disproportionation to form water at ca. 199 K. At temperatures greater than 400 K decarboxylation and decarbonylation of the acetates was seen. The products desorbed were hydrogen, water, carbon monoxide, and carbon dioxide. This is in contrast to acetic acid on the clean Rh(111) surface where water was not observed as a reaction product. These experiments demonstrated that oxygen stabilized the acetates to higher temperatures and participated in the formation of oxidized products.

Acetaldehyde on the Rh(111)–(2 × 2)O Surface

The reaction of acetaldehyde with atomic oxygen also produced surface acetates on Rh(111). Figure 7 is an illus-

TABLE 5

Acetic Acid HREELS Assignments, Frequency (cm^{-1})

Mode	Rh(111)	Rh(111)–(2 × 2)O
$\nu(CH_3)$	2995	2975
ν(OH)	2700/2500	2700
ν(C=O)	1685	1725
$\delta(CH_3)$	1425	1440
ν(C–O)	1310	1325
ν(C–C)	970	980
δ(O–C–O)	630	640

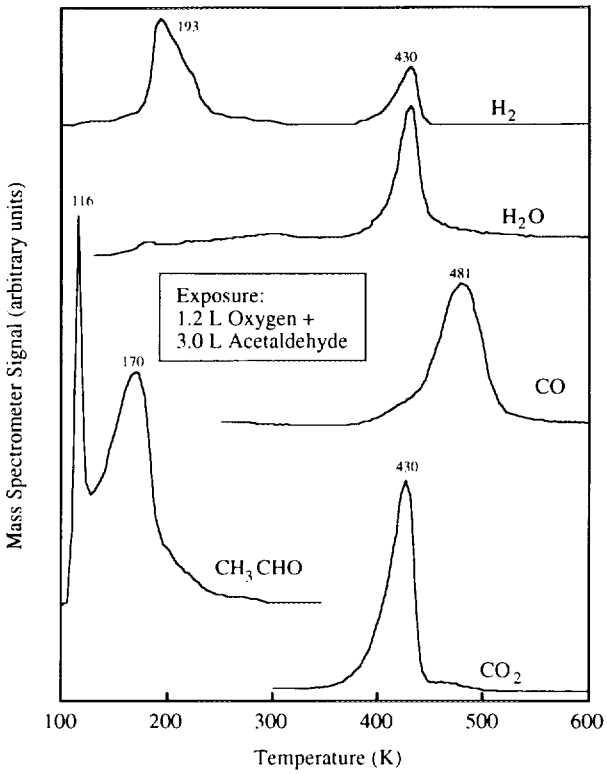

FIG. 7. TPD after an exposure of 3.0 L of acetaldehyde on the Rh(111)–(2 × 2)O surface at 90 K. Yields corresponding to this spectrum are given in Table 6.

tration of the TPD spectrum obtained after exposing an oxygen-dosed Rh(111) surface to 3.0 L of acetaldehyde. The H_2, H_2O, and CO_2 desorption peaks at 430 K were the products of the decomposition of the same intermediate, since they all occurred at the same temperature. As noted above, acetate intermediates generated by acetic acid decomposition on the oxygen-dosed surface decomposed at this temperature, releasing the same volatile products. Thus, as will be confirmed by HREELS, the species responsible for the 430 K desorption peaks was an acetate intermediate formed by the reaction of surface oxygen atoms with acetaldehyde. The TPD yields for the reaction of acetaldehyde on the Rh(111)–(2 × 2)O surface are summarized in Table 6. The ratio of the yield of hydrogen-containing products (H_2 and H_2O), desorbed at 430 K to the yield of CO_2 was 1.5. Thus the stoichiometry of the acetate was preserved. Since no hydrogen-containing products were formed in the vicinity of 300 K that could be attributed to the lower temperature, CO-producing acetate decomposition channel observed for acetic acid on the clean surface, a reaction of an adsorbate other than acetates must be invoked to account for the large amount of CO produced in the reaction of acetaldehyde on the oxygen-dosed surface. It is shown later that a portion of the acetaldehyde decomposed at approximately 200 K and liberated CO which contributed to the peak at 481 K. Additional oxygen atoms reacted with carbon originating from the methyl group of the acetate to form CO, as for the decomposition of acetic acid-derived acetates in the presence of oxygen adatoms. No high-temperature CO or O_2 desorption peaks were observed for the acetaldehyde exposure of Fig. 7, and subsequent oxygen TPD experiments indicated that less than 0.006 ML of carbon remained on the surface after the acetaldehyde TPD experiment. This suggested that carbon atoms from the methyl groups of the acetates were removed during the course of the original experiment. The yields of the other products also were consistent with this explanation. The yield of CO_2 at 430 K gave an estimate of 0.10 ML of acetate decomposed, which implied that 0.10 ML of carbon was released. Thus 67% of the CO desorbed at 481 K could be accounted by the oxidation of the methyl carbon of acetates formed from acetaldehyde and oxygen. The amount of oxygen atoms on the surface also roughly balanced. Approximately 0.3 ML of oxygen was adsorbed on the surface before acetaldehyde adsorption and since 0.12 ML of acetaldehyde decomposed (as determined from the carbon balance) 0.12 ML of oxygen atoms came from acetaldehyde. Oxygen atoms were removed by H_2O, CO and CO_2 production, 0.12, 0.15, and 0.10 ML, respectively.

The desorption of hydrogen produced a peak at 193 K. The peak temperature was consistent with that of hydrogen atoms adsorbed on the oxygen-dosed Rh(111) surface as shown by Thiel *et al.* (46). As noted above, oxidation of acetaldehyde produced 0.10 ML of acetates. From this reaction 0.10 ML of hydrogen atoms must be released to the surface. Since the hydrogen peak was not symmetric, there was likely a reaction producing hydrogen in the range 200–250 K. The amount of H_2 represented by the low-temperature hydrogen peak was 0.09 ML, or 0.18 ML of H atoms; since 0.1 ML of H atoms were produced

TABLE 6

TPD Yields (ML) for an Exposure of 3.0 L of Acetaldehyde on the Rh(111)–(2 × 2)O Surface

CH_3CHO (116 K)	0.045
CH_3CHO (170 K)	0.15
H_2 (193 K)	0.090
H_2 (430 K)	0.026
H_2O (430 K)	0.12
CO_2 (430 K)	0.10
CO (481 K)	0.15
$C_{(ad)}$	<0.006

by the formation of acetates, there was an excess of 0.08 ML of H atoms that could not be attributed to acetate formation. Since, as noted above, 30% of the CO that desorbed at 481 K was not due to acetate decomposition, a fraction of the acetaldehyde appeared to decompose around 250 K. As demonstrated previously (36), decomposition of acetaldehyde occurs in this temperature range on the clean Rh(111) surface.

Molecular acetaldehyde desorbed in two peaks. The low temperature peak at 116 K was consistent with the desorption of multilayer acetaldehyde; the same state was observed for exposures >1.5 L on the clean Rh(111) surface. The higher temperature peak, at 170 K, occurs on the oxygen-dosed Rh(111) surface, but not on the clean surface, and was attributed to acetaldehyde bound in the η^1(O)-configuration. Oxygen adatoms have been shown to favor this configuration for the adsorption of carbonyl-containing molecules (30). This assignment was also confirmed by HREELS experiments described below. The activation energy for the desorption of η^1(O)–acetaldehyde was 42.8 kJ/mol assuming a preexponential factor of 10^{13} s^{-1}. On the clean surface acetaldehyde was observed to polymerize when adsorbed at multilayer coverages (36). These multilayers depolymerized to produce acetaldehyde peaks at 234 and 272 K. No acetaldehyde desorption peaks above 200 K are evident in Fig. 7, and no polymerization was indicated for the 3-L exposure of acetaldehyde on the oxygen-dosed surface. This result is somewhat surprising since preadsorbed oxygen can initiate the polymerization of formaldehyde monolayers on the Rh(111) surface (35).

The HREEL spectra collected after coadsorption of acetaldehyde and oxygen indicated that at least five carbon-containing species were present at various points in the reaction. Figure 8 illustrates the HREEL spectra obtained after exposing the oxygen-dosed surface to 2.0 L of acetaldehyde at 90 K. This exposure produced minimal population of the 116 K multilayer peak in TPD experiments. The 90-K spectrum of Fig. 8 was assigned to oxygen atoms and η^1(O)–acetaldehyde. The loss at 560 cm^{-1} was a combination of the $\nu(M\text{–O})$ mode of atomic oxygen and the δ(C–C–O) mode of acetaldehyde. The intense loss at 1690 cm^{-1} was attributed to the ν(C=O) mode of η^1(O)–acetaldehyde. The frequency of this loss was similar to the gas-phase value of 1722 cm^{-1}. Since bonding to the surface did not significantly reduce the ν(C=O) mode frequency, this species was likely adsorbed via the lone-pair nonbonding electrons on the oxygen. Similar donor bonds have been observed for oxygenates on other transition metal surfaces. The remaining losses in the 90-K spectrum of Fig. 8 were attributed to vibrations associated with the methyl group of η^1(O)–acetaldehyde. These were the $\nu(CH_3)$ mode at 3000 cm^{-1}, the $\delta(CH_3)$ mode at 1390 and 1450 cm^{-1}, the ν(C–C) mode at 1145 cm^{-1}, and the

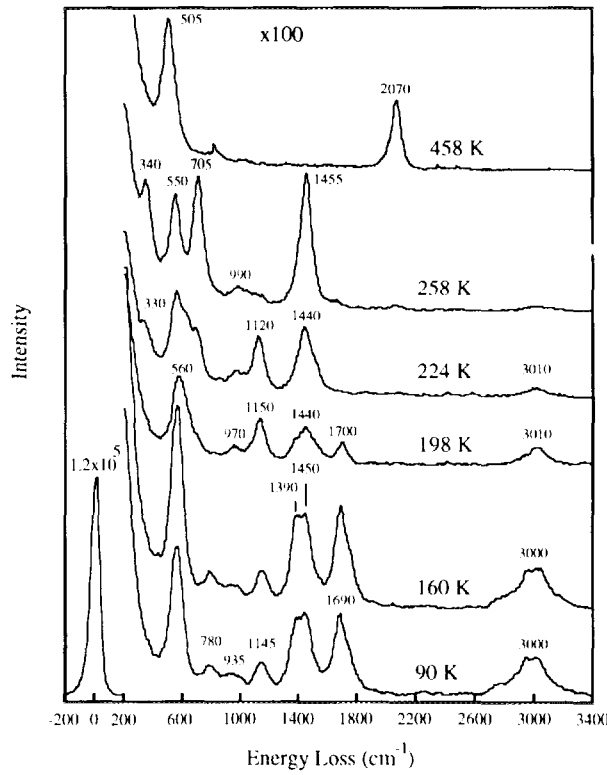

FIG. 8. HREELS after an exposure of 2.0 L of acetaldehyde on the Rh(111)–(2 × 2)O at 90 K, and HREELS after subsequent heating to 160, 198, 224, 258, and 458 K.

$\rho(CH_3)$ mode at 935 cm^{-1}. Table 7 is a summary of the HREELS assignments for η^1(O)–acetaldehyde compared with the frequencies for molecular acetaldehyde and acetaldehyde adsorbed in a multilayer state (36).

The species responsible for the 90-K spectrum persisted without change until 160 K. Between 160 and 198 K the loss assigned to the ν(C=O) mode of η^1(O)–acetaldehyde decreased in intensity. The TPD results described above included the desorption of 0.15 ML of acetaldehyde in a peak at 170 K; therefore, the disappearance of η^1(O)–acetaldehyde from the HREEL spectrum was attributed to

TABLE 7

η^1(O)-Acetaldehyde HREELS Assignments, Frequency (cm^{-1})

Mode	Crystalline (40)	Multilayer on Rh(111) (36)	Rh(111)–(2 × 2)O
$\nu(CH_3)$	2964/2918	3000	3000
ν(C=O)	1722	1745	1690
$\delta(CH_3)$	1431/1389	1450	1450/1390
ν_a(C–C)	1118	1135	1145
$\rho(CH_3)$	882	920	935
δ(C–C–O)	522	545	560

TABLE 8

η^2-Acetaldehyde HREELS Assignments, Frequency (cm^{-1})

Mode	Rh(111) (36)	Rh(111)-(2 × 2)O
$\nu(CH_3)$	2980	3010
$\nu(C{=}O)$	1460	1440
$\delta(CH_3)$	1380	1440
$\nu_a(C{-}C)$	1135	1150
$\rho(CH_3)$	950	970
$\delta(C{-}C{-}O)$	610	560

desorption. The reduction in intensity of the η^1(O)–acetaldehyde losses revealed the presence of another species on the surface. The losses in the 198 K spectrum were primarily associated with the vibrations of methyl groups. These were the $\nu(CH_3)$ mode at 3010 cm^{-1}, the $\delta(CH_3)$ mode at 1440 cm^{-1}, the ν(C–C) mode at 1150 cm^{-1}, and the $\rho(CH_3)$ mode at 970 cm^{-1}. Losses associated with the vibrations of a carbonyl group could not be unambiguously resolved. It was previously observed that η^2(C,O)–acetaldehyde exhibited an intense δ(C–C–O) mode at 610 cm^{-1} and a weaker $\nu(C{=}O)$ mode at 1460 cm^{-1} on the clean Rh(111) surface (36). Thus, the intensities and peak positions of the losses in the 198 K spectrum of Figure 8 were consistent with its assignment to an η^2(C,O)–acetaldehyde, with a small contribution from η^1(O)–acetaldehyde indicated by the loss at 1700 cm^{-1}. A comparison of the frequencies of vibrational modes of η^2(C,O)–acetaldehyde on the clean Rh(111) surface and the oxygen pre-covered Rh(111) surface is shown in Table 8.

Between 198 and 224 K the η^2(C,O)–acetaldehyde began to react with the oxygen to yield acetate species. This reaction was complete by 258 K. Modes characteristic of acetates dominated the 258 K spectrum. Losses corresponding to the ν_s(O–C–O) mode at 1455 cm^{-1}, the δ(O–C–O) mode at 705 cm^{-1}, and the $\nu(M{-}O)$ mode at 340 cm^{-1} were observed, as for acetates produced by acetic acid dissociation, in Fig. 1b. The other loss at 550 cm^{-1} in the 258-K spectrum of Fig. 8 was the $\nu(M{-}O)$ mode of atomic oxygen.

Acetate and oxygen were the only species on the surface between 258 and 350 K. This observation is consistent with the behavior of acetic acid on the oxygen precovered Rh(111) surface. No additional CO was observed to form until the acetate decomposed between 349 and 458 K. CO and oxygen were the only species indicated in the 458-K spectrum of Fig. 8. The loss at 2070 cm^{-1} was the $\nu(C{=}O)$ mode of CO and the loss at 505 cm^{-1} was the combination of the $\nu(M{-}O)$ mode of oxygen and the ν(M–CO) mode of CO. The progress of the reaction of acetaldehyde is summarized in Fig. 9. The normalized integrated intensities of loss peaks associated with various intermediates are plotted versus temperature. The intensities are presented as a percent of the elastic peak intensity. The modes used for this plot were: $\nu(C{=}O)$ at 2070 cm^{-1} for CO, $\nu(C{=}O)$ at 1690 cm^{-1} for η^1(O)–acetaldehyde, ν(C–C) at 1150 cm^{-1} for η^2(C,O)–acetaldehyde, δ(O–C–O) at 705 cm^{-1} for η^2(O, O)–acetate, and $\nu(M{-}O)$ at 500–560 cm^{-1} for oxygen. The loss peak assigned to oxygen had contributions from both the δ(C–C–O) mode of η^1(O)–acetaldehyde and the ν(M–CO) mode of CO. These contributions were removed by subtraction of 35% of the η^1(O)–acetaldehyde intensity at 1690 cm^{-1} and 45% of the CO intensity at 2070 cm^{-1} from the peak at 560 cm^{-1}. The contribution of η^1(O)–acetaldehyde to the apparent intensity of the ν(C–C) mode of η^2(C,O)–acetaldehyde species was difficult to determine and thus was not removed from its intensity. Figure 9 clearly indicates that η^1(O)–acetaldehyde was lost by desorption and conversion to the η^2 state between 160 and 200 K. η^2(C,O)–Acetaldehyde was formed between 160 and 224 K. Between 224 and 258 K, the oxygen and η^2(C,O)–acetaldehyde intensities decreased and the η^2(O,O)–acetate intensity increased. The acetate intensity was lost between 349 and 458 K. The reduction in oxygen intensity and the increase in CO intensity in this same temperature range

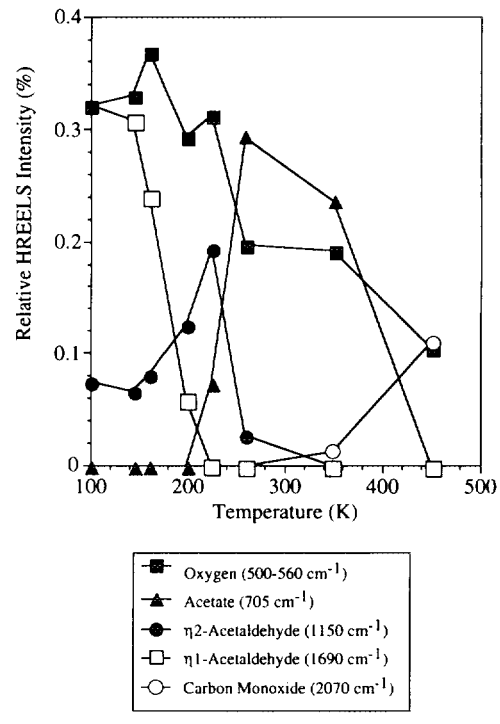

FIG. 9. TPHREELS of the data obtained in the experiments in Fig. 8. The normalized vibrational intensities are plotted versus temperature. The vibrational intensities were expressed as a percentage of the intensity of the elastic peak.

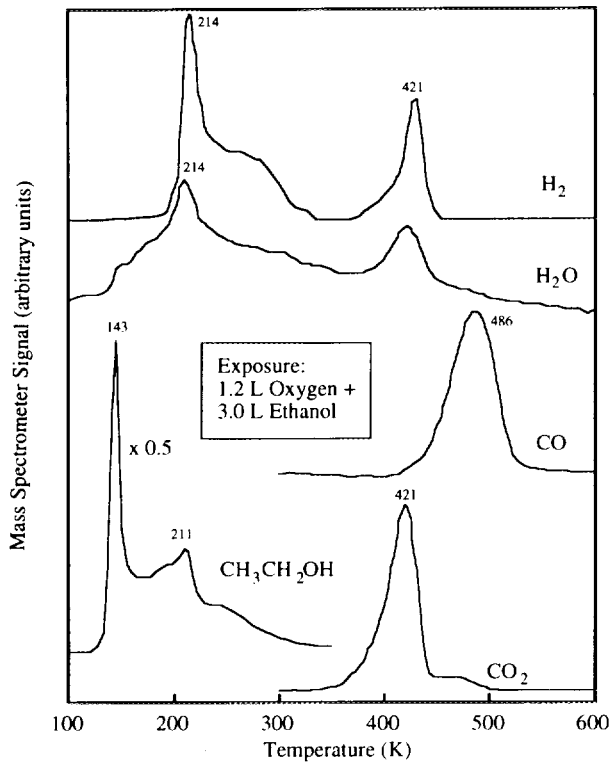

FIG. 10. TPD after an exposure of 3.0 L of ethanol on the Rh(111)–(2 × 2)O surface at 90 K. Yields corresponding to this spectrum are given in Table 9.

indicated that CO may have been formed by oxidation of the carbon-containing groups, e.g., the methyl moiety of the acetate intermediate, although some of the oxygen atoms on the surface were also consumed by reaction with hydrogen atoms to produce water.

Ethanol on the Rh(111)–(2 × 2)O Surface

Above 300 K the behavior of ethanol on the oxygen-dosed surface was very similar to that of acetaldehyde shown in the TPD data of Fig. 7. The TPD spectrum in Fig. 10 was obtained after exposing the (2 × 2)O surface to 3.0 L of ethanol. The H_2, H_2O, and CO_2 peaks characteristic of acetate decarboxylation on the oxygen-dosed Rh(111) surface were observed at 421 K. The slight reduction in decomposition temperature of the acetate produced from ethanol oxidation versus the acetate produced by acetaldehyde oxidation was the result of the lower oxygen atom coverage remaining on the surface upon completion of acetate formation from the more hydrogen-rich reactant, ethanol. Oxygen was removed in the course of the reaction of ethanol by formation and desorption of water at 214 K. The ratio of hydrogen-containing products, H_2 and H_2O, to CO_2 represented by the peaks at 421 K was 1.3, which is roughly consistent with the stoichiometry of acetate. The yields for the spectrum in Fig. 10 are summarized in Table 9. Since very little carbon remained on the surface after the TPD experiment, at least some of the carbon atoms contained in the molecular CO desorbing at 486 K must have originated from the methyl groups of the acetates decomposed at lower temperature. Similar chemistry was also indicated after acetaldehyde adsorption on the oxygen-dosed surface, as discussed above. The desorption of ethanol from the oxygen-dosed Rh(111) surface was also qualitatively similar to the desorption of acetaldehyde after the adsorption of acetaldehyde. A peak characteristic of desorption from a multilayer state occurred at 143 K. The peak at 211 K was attributed to molecular ethanol bound via the lone pair electrons on the oxygen atom. The recombination of alkoxides with hydrogen atoms to produce the parent alcohol has also been proposed to occur on transition metal surfaces (48); however, we have shown by the coadsorption of deuterium and methanol that the recombination made only a minor contribution to the desorption of methanol near 200 K (34). Since similar desorption temperatures for these two alcohol desorption processes have been observed on clean Rh(111) (36) and Pt(111) surfaces (48), the presence of oxygen atoms did not appear to alter significantly the characteristics of ethanol-surface interactions.

The ethanol and acetaldehyde TPD results differed in the low temperature desorption of water and hydrogen. As noted above, atomic hydrogen recombines and desorbs from the oxygen-dosed Rh(111) surface at ca. 200 K, near its peak temperature of 214 K in Fig. 10. Thus the production of atomic hydrogen from ethanol on this surface must have occurred at or below this temperature, Thiel *et al.* (46) have reported that for coadsorbed atomic hydrogen and oxygen on Rh(111) small amounts of water are formed and that these appear at ca. 300 K in TPD experiments. Thus, the water desorbed at 214 K in Fig. 10 was attributed to the reaction of hydroxyls and atomic hydrogen. These hydroxyl groups were formed by hydro-

TABLE 9

TPD Yields (ML) for an Exposure of 3.0 L of Ethanol on the Rh(111)–(2 × 2)O Surface

C_2H_5OH (143 K)	0.021
C_2H_5OH (211 K)	0.081
H_2 (216 K)	0.092
H_2 (421 K)	0.032
H_2O (212 K)	0.08
H_2O (421 K)	0.031
CO_2 (421 K)	0.051
CO (481 K)	0.093
$C_{(ad)}$	0.01

gen transfer from the ethanol hydroxyl group to surface oxygen. Since the production of water at this temperature was not observed for acetaldehyde adsorbed under the same conditions, other sources of water formation were not likely. The direct transfer of hydroxyl hydrogens is characteristic of alcohols adsorbed on oxygen-dosed transition metals. By the use of isotopically labelled methanol, Davis and Barteau (49) have shown that this reaction occurs on the oxygen-dosed Pd(111) upon adsorption at 170 K, and the subsequent reaction of hydrogen atoms with surface hydroxyls occurs at 240 K. The higher temperature shoulder on the hydrogen desorption peak in Fig. 10 indicated that a reaction producing hydrogen atoms occurred between 220 and 300 K. Since the production of acetates accounts for only 0.15 ML of the H atoms desorbed below 300 K, there was an excess of hydrogen detected that likely was the result of another reaction-producing hydrogen and CO on the surface between 200 and 300 K. However, identification of this reaction pathway was not possible with TPD experiments alone. There were no other products such as acetaldehyde, ketene or methane desorbed during the ethanol TPD experiments. In summary, except for the transfer of the hdyroxyl hydrogen to surface oxygen atoms, the TPD spectrum after exposing the oxygen-dosed surface to ethanol was very similar to the spectrum obtained after acetaldehyde adsorption.

The HREEL spectra confirmed that the dominant intermediates produced from ethanol on the oxygen-predosed surface above 200 K were identical to those produced from acetaldehyde. As expected, however, the spectrum upon adsorption at 90 K was different. The losses in the 90 K spectrum of Fig. 11 were largely due to an ethoxide or ethanol intermediate. A summary of the HREELS assignments for ethanol and ethoxide is given in Table 10. the assignment as ethoxide was favored by the low intensity of OH modes, expected at 815 and 3270 cm^{-1} on the basis of HREELS spectra collected after the adsorption of ethanol on the clean surface (36); however, these O–H modes are expected to be weak and it was likely that molecular ethanol also existed on the surface until 211 K where it was observed to desorb in TPD. The modes at 895, 1480, and 3010 cm^{-1} were the vibrations of the methyl and methylene moieties of the ethoxide or ethanol. The ν(C–O) mode was assigned to the loss at 1065 cm^{-1}. The loss at 580 cm^{-1} was due to the $\nu(M\text{–O})$ mode of atomic oxygen. A decrease in intensity of both the oxygen and ethanol/ethoxide vibrational modes was observed to occur between 140 and 239 K. This was consistent with the desorption of ethanol and water observed in the TPD experiments. The 239 K spectrum of Fig. 11 was very similar to the 224 K spectrum of Fig. 8. This indicated that the same intermediates were produced by the dehydrogenation of ethanol and acetaldehyde on the oxygen-dosed Rh surface. As noted above, the vibrational spectra indicated that an η^2(C,O)–acetaldehyde species was a likely candidate. The decrease in intensity of the loss at 545 cm^{-1} indicated that oxygen was consumed by the

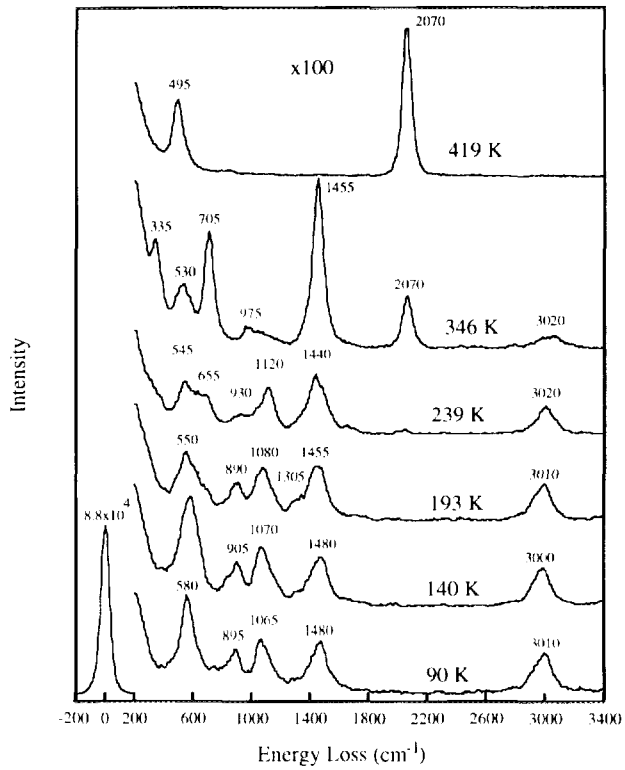

FIG. 11. HREELS after an exposure 1.5 L of ethanol on the Rh(111)–(2 × 2)O surface at 90 K, and HREELS after subsequent heating to 140, 193, 239, 346, and 419 K.

TABLE 10

Ethanol and Ethoxide HREELS Assignments, Frequency (cm^{-1})

	Ethanol		Ethoxide	
Mode	Solid (40)	Rh(111) (36)	Rh(111) (36)	Cu (50)
ν(OH)	3676	3270	—	—
$\nu(CH_3)$	2989/2943	2990	2990	2970/2860
$\nu(CH_2)$	2900	nr	nr	nr
$\delta(CH_2)$	1490	1490	1405	1450
$\delta(CH_3)$	1452/1394	1380	1390	1380
γ(OH)	1241	815	—	—
ν_a(C–C–O)	1089	1070	1070	1030
$\rho(CH_3)$	1033	nr	nr	nr
ν_s(C–C–O)	885	890	880	870
$\gamma(CH_2)$	801	815	nr	nr
δ(C–C–O)	419	480	510	470

Note. nr, not resolved.

production of water after ethanol adsorption. Since acetaldehyde does not have a hydroxyl hydrogen, this avenue for oxygen consumption was not observed for that molecule. After the formation of the acetaldehyde intermediate from ethanol, its subsequent reaction intermediates and the temperatures of these conversions were nearly identical to those described for acetaldehyde decomposition. Losses characteristic of acetate dominated the 346 K spectrum of Fig. 11, and CO was the primary species remaining on the surface at 419 K.

In summary, the TPD and HREEL spectra obtained after the adsorption of ethanol and acetaldehyde on the oxygen-dosed surface were very similar. Both oxygenates produced η^2(C,O)–acetaldehyde intermediates between 160 and 220 K. These acetaldehyde intermediates reacted with surface oxygen to produce acetates. The decarboxylation of acetates occurred at ca. 430 K. The products desorbed at this temperature were hydrogen, water and carbon dioxide. The major difference between the reactions of ethanol and acetaldehyde was the desorption of water at 214 K from ethanol only. This water was due to the reaction of hydroxyls and atomic hydrogen. The hydroxyls were formed by direct transfer of the hydroxyl hydrogens of ethanol to surface oxygen atoms.

DISCUSSION

On the Rh(111)–(2 × 2)O surface the decomposition sequence of ethanol included acetaldehyde as an intermediate. Above 220 K the TPD and HREEL spectra of the ethanol- and acetaldehyde-derived layers were identical. The existence of a pathway for ethanol decomposition that included acetaldehyde was quite different from results for ethanol decomposition on the clean Rh(111) surface (36). Without oxygen atoms on the Rh(111) surface the ethoxide intermediate did not dehydrogenate to a significant extent to acetaldehyde as it does on clean Ni(111) (51) and Pd(111) (52); instead, C–H bond cleavage at the methyl group initiated complete dehydrogenation that ultimately resulted in carbon deposition and CO formation. The formation of acetaldehyde intermediates from ethanol on the oxygen-dosed surface indicated that dehydrogenation at the α position became favored in the presence of oxygen. The cause of this shift in selectivity was not clear; however, the subtlety of the factors controlling the selectivity of ethoxide decomposition was also indicated by the striking difference in ethoxide decomposition pathways between two metal surfaces adjacent in the periodic table, Rh(111) and Pd(111).

Adsorbed oxygen atoms promoted the formation of ethoxide intermediates on both Rh(111) and Rh(110) (53). The direct transfer of hydroxyl hydrogens to surface oxygen atoms has been reported on many surfaces (51, 52, 54). The desorption of water at 200 K was characteristic of coadsorption of oxygen and alcohols on the Rh(111) surface. Similar water desorption peaks have been previously reported for methanol adsorbed on the oxygen-dosed Rh(111) surface (34). This water was the result of the reaction of atomic hydrogen and hydroxyls bonded to the surface.

The influence of adsorbed oxygen atoms was also manifested in the shift of the preferred bonding configuration of acetaldehyde upon adsorption from η^2(C,O) to η^1(O). This result was not surprising since the electronic influence of the oxygen has been shown to cause the same shift in the bonding configuration of acetone on Ru(0001) (55), Rh(111) (31), and Pd(111) (30). The binding of acetaldehyde in this configuration reduced its tendency to decompose. On the clean Rh(111) surface the first layer of acetaldehyde decomposed completely (36) while on the oxygen-dosed surface approximately 50% of the acetaldehyde adsorbed in the first layer desorbed without reaction. The mechanism of acetaldehyde decomposition was also modified by oxygen atoms. On the clean surface acetaldehyde decarbonylated to produce methyl groups and CO molecules on the surface. Apparently the presence of oxygen on the Rh(111) surface blocked this methyl migration; instead η^2(C,O)–acetaldehyde reacted with surface oxygen atoms to produce adsorbed acetate intermediates.

Since a nearly universal feature of formic acid adsorption on late transition metal surfaces is the production of stable formate intermediates, it is not surprising that acetate intermediates were easily isolated following acetic acid adsorption. The formate on the initially clean Rh(111) surface decomposed between 225 and 290 K (45). This temperature can be compared to that for the decarboxylation of acetates on Rh(111), 372 K. This stability difference between acetates and formates is in accord with those observed on other Group VIII metals, including Pd (39), Ni (56), and Fe (57). The influence of oxygen atoms also resulted in greater stability of acetate species on the Rh(111)–(2 × 2)O surface. Decarboxylation on the Rh(111)–(2 × 2)O surface occurred at 433, 430, and 421 K for acetates derived from acetic acid, acetaldehyde, and ethanol, respectively, reflecting the variation in the oxygen atom coverage remaining after acetate synthesis from each. The fragmentation of the carboxyl group of the acetate to release CO and atomic oxygen was indicated on the Rh(111) surface. The selectivity to this mode in the case of formate decomposition depends on the identity of the metal surface. For example, Cu (58) and Ag (59) exhibit only decarboxylation of formate to CO_2 while Rh (35), Ni (60), and Pd (61) exhibit both decarboxylation and C–O bond scission. These trends for formate decomposition appear to extend to acetate decomposition. While acetate decomposition on Cu (42) did not result in any CO formation, Rh, Ni (56), and Pd (39) all showed significant production of CO from acetate intermediates. Some cau-

tion must be exercised in making this comparison since acetate decomposition liberates ketene ($H_2C{=}C{=}O$) on the Group Ib metals (42), ketene has not been detected from acetates on the Group VIII metals, but it could still provide a route to CO if its decomposition is rapid on those metals. On oxygen-covered Rh(110), the acetate decomposes via "explosive kinetics" (53). This is the first observation of this phenomenon on Rh. The products of this explosion were CO_2 and H_2 from decomposition of the acetate formed from acetic acid dehydrogenation. For the acetate formed via ethanol oxidation, the products of this explosion depended on the ethanol exposure. At high exposures coincident CO_2 and H_2 evolution was observed from TPD studies, while at low doses coincident evolution of CO_2 and H_2O was observed.

Since oxygen atoms present on the surface of supported catalysts did not exchange with the oxygen atoms supplied by the reactants, Naito *et al.* (9) concluded that the oxygen atoms of the acetate formed were not equivalent. The oxygen atoms of acetates on the Rh(111) surface were completely equivalent. Thus the present results suggest that the inequivalence of acetate oxygens in the catalysis experiments requires that oxygen atoms supplied on the supported catalyst must be bonded to another element, and cannot be free oxygen atoms on the metal surface. The explanation advanced by Naito *et al.* (9) was that the oxygen supplied by the catalyst was bound to sodium atoms, or in some other unidentified state in the case of TiO_2-supported catalysts, and was not simply adsorbed on the transition metal surface.

The results of this study support the conclusion of Naito *et al.* (9) that a reaction pathway connects acetates with acetaldehyde and ethanol on supported rhodium catalysts. Acetates were readily formed after the adsorption of both ethanol and acetaldehyde on the oxygen-containing Rh(111) surface and on supported catalysts (9, 10). The reverse of this acetate formation is a possible mechanism for ethanol and acetaldehyde formation as proposed by Bowker (11). The existence of such a carboxylate pathway for oxygenate synthesis may lead to the difficulty in identifying the ethanol synthesis pathway on supported Rh catalysts. Underwood and Bell have concluded that Rh supported on La_2O_3 hydrogenated acetaldehyde to ethanol (62), while Jackson *et al.* have reported that for Rh supported on SiO_2 ethanol was not produced via a pathway that included acetaldehyde (63). Since La_2O_3 tends to interact with the metal surface much like TiO_2, while SiO_2 is a relatively inert support, different mechanisms may be responsible for the results on these two catalysts. Based on the observations of Naito *et al.* (9) and Orita *et al.* (10) and the single-crystal results, one would expect carboxylates to play a more prominent role for metal catalysts supported on interacting rather than noninteracting oxides. Thus interpretation of the results of studies intended to elucidate the pathway of ethanol formation on supported metal catalysts may be complicated by the existence of multiple pathways, as recognized by "interconnected" mechanistic schemes such as that of Bowker (11). The relative importance of these different routes will depend on metal, support, promoters, etc. Unfortunately, the commonality of reaction products to different pathways renders the connection of product selectivity to mechanism, and thence to catalyst properties, a difficult proposition.

CONCLUSIONS

From TPD and HREELS experiments it was shown that acetates are produced during the decomposition of acetic acid, acetaldehyde, and ethanol on the Rh(111)–(2 × 2)O surface. Acetates formed from acetic acid on Rh(111) decomposed via carboxylation to liberate CO_2 and H_2, as well as by C–O scission to release CO and atomic oxygen. Acetic acid and ethanol on the oxygen-dosed surface reacted via direct hydrogen transfer to surface oxygen atoms to form surface hydroxyls; these reacted with hydrogen atoms to form water at ca. 200 and 214 K, respectively. The formation of water at low temperatures did not occur during the conversion of acetaldehyde to acetate. Adsorbed oxygen also stabilized the surface acetates such that increased thermal energy was necessary to facilitate decomposition. Most importantly, ethanol and acetaldehyde on Rh(111)–(2 × 2)O were oxidized to acetates via a common intermediate, η^2(C,O) acetaldehyde, in direct contrast to their behavior on clean Rh(111) where no common pathway was detected. These observations again suggest that reaction pathways and intermediates involved in oxygenate synthesis are dependent upon the metal, support, and the promoter used. The existence of multiple routes to common products renders selectivity a poor probe of mechanism in oxygenate synthesis catalysis.

ACKNOWLEDGMENT

We gratefully acknowledge the support of this research by the Department of Energy, Office of Basic Energy Sciences, Division of Chemical Sciences (Grant FG02-84ER13290).

REFERENCES

1. Madix, R. J., *Adv. Catal.* **29,** 1 (1980).
2. Barteau, M. A., *Catal. Lett.* **8,** 175 (1991).
3. Rootsaert, W. J. M., and Sachtler, W. M. H., *Z. Phys. Chem.* **26,** 16 (1960).
4. Van Herwijnen, T., and de Jong, W. A., *J. Catal.* **63,** 83 (1980).
5. Rethwisch, D. G., and Dumesic, J. A., *Appl. Catal.* **21,** 97 (1986).
6. Kung, H. H., "Transition Metal Oxides: Surface Chemistry and Catalysis," p. 245. Elsevier, Amsterdam, 1989.
7. Millar, G. J., Rochester, C. H., Bailey, S., and Waugh, K. C., *J. Chem. Soc. Faraday Trans.* **88,** 2085 (1992).

8. Shustorovich, E., and Bell, A. T., *Surf. Sci.* **253,** 386 (1991).
9. Naito, S., Yoshioka, H., Orita, H., and Tamaru, K., *in* "Proceedings, 8th International Congress on Catalysis, Berlin, 1984," Vol. 3, p. 267. Dechema, Frankfurt-am-Main, 1984.
10. Orita, H., Naito, S., and Tamaru, K., *J. Catal.* **90,** 183 (1984).
11. Bowker, M., *Catal. Today,* **15,** 77 (1992).
12. Van der Lee, G., Bastein, A., Van der Boogert, J., Schuller, B., Luo, H., and Ponec, V., *J. Chem. Soc. Faraday Trans. 1* **83,** 2103 (1987).
13. Force, E. L., and Bell, A. T., *J. Catal.* **44,** 175 (1976).
14. Ai, M., *Catal. Today,* **13,** 679 (1992).
15. Kim, K. S., and Barteau, M. A., *J. Catal.* **125,** 353 (1990).
16. Sugiyama, S., Sato, K., Yamaski, S., Kawashiro, K., and Hayashi, H., *Catal. Lett.* **14,** 127 (1992).
17. Bailey, O. H., Montag, R. A., and Yoo, J. S., *Appl. Catal. A* **88,** 163 (1992).
18. Iglesia, E., and Boudart, M., *J. Phys. Chem.* **95,** 7011 (1991).
19. Nakamura, J., Campbell, J. M., and Campbell, C. T., *J. Chem. Soc. Faraday Trans.* **86,** 2725 (1990).
20. Campbell, C. T., and Daube, K. A., *J. Catal.* **104,** 109 (1987).
21. Ovesen, C. V., Stoltze, P., Norskov, J. K., and Campbell, C. T., *J. Catal.* **134,** 445 (1992).
22. Kikuzono, Y., Kagami, S., Naito, S., Onishi, R., and Tamaru, K., *Faraday Discuss. Chem. Soc.* **72,** 135 (1982).
23. Driessen, J. M., Poels, E. K., Hindermann, J. P., and Ponec, V., *J. Catal.* **82,** 26 (1983).
24. Rieck, J. S., and Bell, A. T., *J. Catal.* **96,** 88 (1985).
25. Deligianni, H., Mieville, R. L., and Peri, J. B., *J. Catal.* **95,** 465 (1985).
26. Berlowitz, P. J., and Goodman, D. W., *J. Catal.* **108,** 364 (1987).
27. Logan, A. D., Braunschweig, E. J., Datye, A. K., and Smith, D. J., *Langmuir* **4,** 827 (1988).
28. Solymosi, F., Tambácz, I., and Kocsis, M., *J. Catal.* **75,** 78 (1982).
29. Erdöhelyi, A., Pásztor, M., and Solymosi, F., *J. Catal.* **98,** 166 (1986).
30. Davis, J. L., and Barteau, M. A., *Surf. Sci.* **208,** 383 (1989).
31. Houtman, C., and Barteau, M. A., *J. Phys. Chem.* **95,** 3755 (1991).
32. Thiel, P. A., Williams, E. D., Yates, J. T., Jr., and Weinberg, W. H., *Surf. Sci.* **84,** 54 (1979).
33. Ko, E. I., Benziger, J. B., and Madix, R. J., *J. Catal.* **62,** 264 (1980).
34. Houtman, C., and Barteau, M. A., *Langmuir* **6,** 1558 (1990).
35. Houtman, C., and Barteau, M. A., *Surf. Sci.* **248,** 57 (1991).
36. Houtman, C., and Barteau, M. A., *J. Catal.* **130,** 528 (1991).
37. Brown, N. F., and Barteau, M. A., *Langmuir* **8,** 862 (1992).
38. Brown, N. F., and Barteau, M. A., *J. Am. Chem. Soc.* **114,** 4258 (1992).
39. Davis, J. L., and Barteau, M. A., *Langmuir* **5,** 1299 (1989).
40. Shimanouchi, T., "Tables of Molecular Vibrational Frequencies, Part 1." National Bureau of Standards, Washington DC, 1972.
41. Surman, M., Lackey, D., and King, D. A., *J. Electron. Spectrosc. Relat. Phenom.* **39,** 245 (1986).
42. Bowker, M., and Madix, R. J., *Appl. Surf. Sci.* **8,** 299 (1981).
43. Jones, L. H., and McLaren, E., *J. Chem. Phys.* **22,** 1795 (1954).
44. Brown, N. F., and Barteau, M. A., *Surf. Sci.*, in press.
45. Solymosi, F., Kiss, J., and Kovács, I., *Surf. Sci.* **192,** 47 (1987).
46. Thiel, P. A., Yates, J. T., Jr., and Weinberg, W. H., *Surf. Sci.* **90,** 121 (1979).
47. Sault, A. G., and Madix, R. J., *Surf. Sci.* **172,** 598 (1986).
48. Sexton, B. A., Rendulic, K. D., and Hughes, A. E., *Surf. Sci.* **121,** 181 (1982).
49. Davis, J. L., and Barteau, M. A., *Surf. Sci.* **197,** 123 (1988).
50. Sexton, B. A., *Surf. Sci.* **88,** 299 (1979).
51. Gates, S. M., Russell, J. N., and Yates, J. T., Jr., *Surf. Sci.* **171,** 111 (1986).
52. Davis, J. L., and Barteau, M. A., *Surf. Sci.* **235,** 235 (1990).
53. Bowker, M., and Li, Y., *Catal. Lett.* **10,** 249 (1991).
54. Solymosi, F., Tarnóczi, T. I., and Berkó, A., *J. Phys. Chem.* **88,** 6170 (1984).
55. Anton, A. B., Avery, N. R., Toby, B. H., and Weinberg, W. H., *J. Am. Chem. Soc.* **108,** 684 (1986).
56. Schoofs, G. R., and Benziger, J. B., *Surf. Sci.* **143,** 359 (1984).
57. Benziger, J. B., and Madix, R. J., *J. Catal.* **65,** 49 (1980).
58. Bowker, M., and Madix, R. J., *Surf. Sci.* **102,** 542 (1981).
59. Sexton, B. A., and Madix, R. J., *Surf. Sci.* **105,** 177 (1981).
60. Benziger, J. B., and Schoofs, G. R., *J. Phys. Chem.* **88,** 4439 (1984).
61. Davis, J. L., and Barteau, M. A., *Surf. Sci.* **256,** 50 (1991).
62. Underwood, R. P., and Bell, A. T., *Appl. Catal.* **21,** 157 (1986).
63. Jackson, S. D., Brandreth, B. J., and Winstanly, D., *J. Catal.* **106,** 464 (1987).